

Electrochemical Behavior of Pristine Mn₂O₃ Efficient Electrodes by Inexpensive Potentiostatic Electrodeposition Technique

S.G. Pawar¹, C.V. Chanmal¹, S.S. Bandgar¹, R.N. Mulik¹, P.A. Desai², A.A. Admuth², I.A. Dhole^{3,*}

¹ Department of Physics, D.B.F. Dayanand College of Arts and Science, 413002 Solapur, (M.S.), India

² Department of Physics, Smt. Kasturba Walchand College, 416416 Sangli, (M.S.), India

³ Department of Physics, Sadguru Gadage Maharaj College, 415124 Karad, (M.S.), India

(Received 16 December 2021; revised manuscript received 19 April 2022; published online 29 April 2022)

Mn₂O₃ nanoflake type electrode for supercapacitor applications has been successfully electrodeposited on stainless steel (SS) current collector by potentiostatic way without using any binder or capping agent. Structural, morphological and compositional properties of the prepared Mn₂O₃ electrodes were characterized using X-ray diffraction (XRD), field emission scanning electron microscopy (FESEM) and Fourier transform infra-red (FTIR) spectroscopy techniques, respectively. The XRD study revealed Mn₂O₃ nanoparticles exhibiting body centered cubic (BCC) crystal structure confirmed using JCPDS no. 89-2809. The FESEM images show nanoflake, lamellar and porous morphology suitable for electrochemical applications. The formation of Mn₂O₃ was confirmed using FTIR spectra. The electrochemical performance of Mn₂O₃ electrode was investigated using cyclic voltammetry (CV), galvanostatic charge discharge (GCD) and electrochemical impedance spectroscopy (EIS) in Na₂SO₄, NaOH and KCl electrolytes. It is revealed that the 1 M Na₂SO₄ electrolyte is well suited for Mn₂O₃ nanoflake type electrode for supercapacitor applications exhibiting specific capacitance (C_{sp}) of 508 Fg⁻¹ at a scan rate of 5 mVs⁻¹. The better C_{sp} values may be due to large active sites and rapid ionic transport across the Mn₂O₃ electrode's surface. Analysis of the electrochemical stability of the Mn₂O₃ electrode exhibits a capacity retention value of 83 % after 1000 cycles in 1 M Na₂SO₄ electrolyte at a scan rate of 100 mVs⁻¹.

Keywords: Mn₂O₃, Cyclic voltammetry, Supercapacitor, Electrodeposition.

DOI: 10.21272/jnep.14(2).02002

PACS numbers: 81.15.Pq, 82.47.Uv

1. INTRODUCTION

The changing lifestyle of human beings, industrialization has increased the demand for energy. The scientific community therefore is continuously directing their efforts in developing energy storage devices. One such device, the supercapacitor, has emerged out as potential candidate of energy storage device family. The advantages of supercapacitors over battery storage devices are high power density, large charging-discharging cycles, long life, and fast charging [1]. Supercapacitors found applications in energy recapture sources such as forklifts, load cranes and electric vehicles, power quality improvement etc. [2]. In general, the supercapacitors are categorized as electrical double layer capacitor (EDLC), pseudocapacitor and hybrid supercapacitors. In EDLC, the charges are stored on the electrode electrolyte interface electrostatically. The capacitance in this case depends on the surface area of electrode. In pseudocapacitors, reversible faradic reactions take place between electrode and electrolyte. The hybrid supercapacitors are the combination of both EDLC and pseudocapacitors. Electrodes in supercapacitors play a key role, hence the choice of the proper electrode material is very important [3]. Compared to EDLCs, pseudocapacitors feature a rapid and desired reversible redox reaction that supports a good charging and discharging process, resulting in increased charge storage capacities. Furthermore, because of their quick energy collection, high energy, and high-power delivery, pseudocapacitors are an excellent storage solution for rechargeable batteries. The active electrodes of

supercapacitors are typically made of carbon-based materials, conducting polymers, and a range of transition metal oxide compounds such as NiO, Fe₂O₃, SnO₂, MnO₂ and Mn₂O₃ [4].

Manganese-based oxides (MnO_x) and their derivatives, such as MnO₂, Mn₂O₃, and Mn₃O₄, are commonly utilized as electrode materials in supercapacitors because of their non-toxicity, good structural flexibility and high chemical and physical stability in a variety of electrolytes [5]. Mn₂O₃ compounds, in particular, have exhibited excellent specific capacitance as anode materials in lithium-ion batteries. Mn₂O₃ based electrodes in supercapacitors have received less attention till now, but they are anticipated to have high capacity and storing qualities, and superior environmental friendliness [6]. Various alterations, including chemical modifications, the insertion of high surface-area conductive materials, and nanostructure creation, have all been used to increase the performance of Mn₂O₃ based electrodes. It is vital to adjust the electrodeposition process parameters in order to maximize the specific capacitance and cycling stability of the prepared electrode [7]. Conventionally supercapacitors require a binder for coating the active material on the current collector, which boosts the electrode's internal resistance while also increasing the device's volume and cost [8].

In the present work, Mn₂O₃ nanoflake type electrodes were successfully synthesized using the potentiostatic electrodeposition method on stainless steel (SS) current collector without any binder or capping agent. We systematically studied the electrochemical properties of Mn₂O₃ electrodes in Na₂SO₄, NaOH and KCl

* iadhole@gmail.com

electrolytes. The Mn_2O_3 nanoflake type electrode in 1 M Na_2SO_4 solution has excellent electrochemical performance bearing specific capacitance of 508 Fgm^{-1} at a scan rate of 5 mVs^{-1} , specific energy of 44.72 Wh/kg , specific power of 41.66 kW/kg and electrochemical stability of 83 % after 1000 cycles.

2. EXPERIMENTAL DETAILS

Manganese acetate tetrahydrate ($\text{Mn}(\text{CH}_3\text{COO})_2 \cdot 4\text{H}_2\text{O}$), sodium sulphate (Na_2SO_4), sodium hydroxide (NaOH) and potassium chloride (KCl) were purchased from Merck. All reagents used were of analytical grade and used without further purification. Double distilled water was used in the synthesis process. This SS 304 plate was cut into pieces of $1 \times 5 \text{ cm}^2$ and polished with sic paper and then degreased with double distilled water. The SS pieces were kept in ultrasonic bath for 30 min to remove surface oxides. Afterwards they were rinsed with double distilled water and dried in air to be used as substrates.

0.1 M manganese acetate precursor solution was prepared using manganese acetate tetrahydrate $\text{Mn}(\text{CH}_3\text{COO})_2 \cdot 4\text{H}_2\text{O}$. During synthesis no other chemicals were added in the precursor solution. The potentiostatic electrodeposition method was carried using a constant voltage source in a two-electrode electrochemical system consisting of SS 304 as the working electrode and graphite as the counter electrode, as shown in Fig. 1. The constant voltage applied was optimized to be 1.7 V for 20 min deposition time. The obtained thin films were annealed at a temperature of 500°C for 1 h to form Mn_2O_3 electrodes.

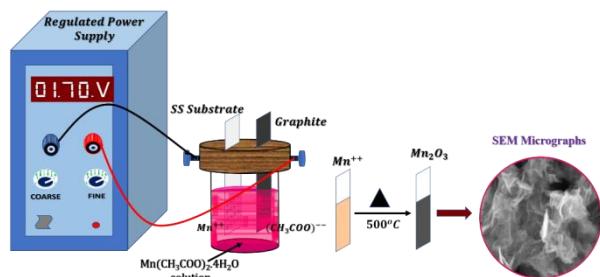


Fig. 1 – Schematic representation of preparation of nanoflake type potentiostatically deposited Mn_2O_3 electrodes

The structural properties of potentiostatically deposited Mn_2O_3 supercapacitor electrode were studied by X-ray diffraction (XRD), Ultima IV, Japan with $\text{CuK}\alpha$ radiation ($\lambda = 1.5406 \text{ \AA}$) in 2θ range of 10° to 80° . The microscopic analysis was carried out by field emission scanning electron microscopy (FESEM), FE-SEM MIRA3 TESCAN to explore the surface morphology of the prepared electrode. The confirmation of the chemical structure of electrodes was done with Fourier transform infra-red (FTIR), Nicolet iS20 spectroscopy in the 500 to 4000 cm^{-1} wavenumber range. The mass of active substance on the electrode was measured using a high precision analytic balance (CONTECH, with 0.01 mg sensitivity). The electrochemical experiments of Mn_2O_3 electrodes were conducted on a CH Instrument's Electrochemical Workstation (CH608E) in a three-electrode system, consisting of Mn_2O_3 , platinum

wire and saturated calomel electrode (SCE) as working, counter and reference electrodes, respectively, in 1 M Na_2SO_4 , 1 M NaOH , and 1 M KCl electrolytes.

3. RESULTS AND DISCUSSION

The crystalline behavior of potentiostatically deposited Mn_2O_3 film was determined via X-ray diffraction pattern, as shown in Fig. 2. The well-defined peaks at $23.1, 32.9, 38.1, 40.6, 45.1, 49.2, 55.1$ and 65.6 are indexed to (211), (222), (400), (411), (332), (431), (440) and (622) planes, respectively. All the observed diffraction peaks are consistent with the JCPDS no. 89-2809 of bixbyite synthetic BCC crystal and space group $\text{Ia}\bar{3}$, lattice constants $a = b = c = 9.4 \text{ \AA}$. The crystallite size of the synthesized Mn_2O_3 was determined by the Debye-Scherrer relation [9]:

$$CS = \frac{0.9\lambda}{\beta \cos \theta} \quad (1)$$

where β is the full width at half maximum (FWHM) of the diffraction peak, k is the shape factor, usually equal to 0.9, and λ is the X-ray wavelength used in XRD. The crystallite size of Mn_2O_3 was found equal to 17.27 nm using the Debye-Scherrer relation.

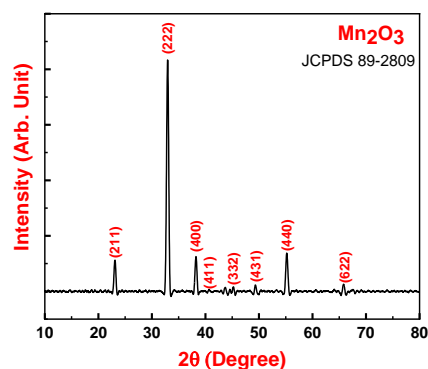
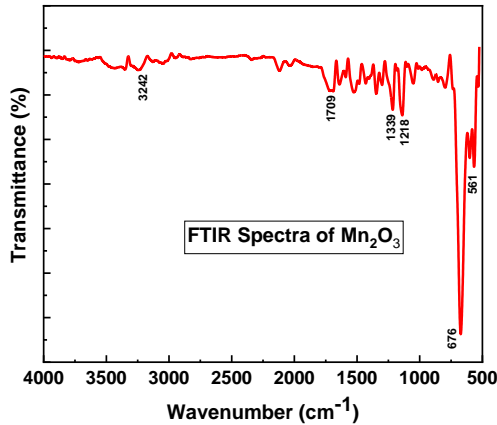
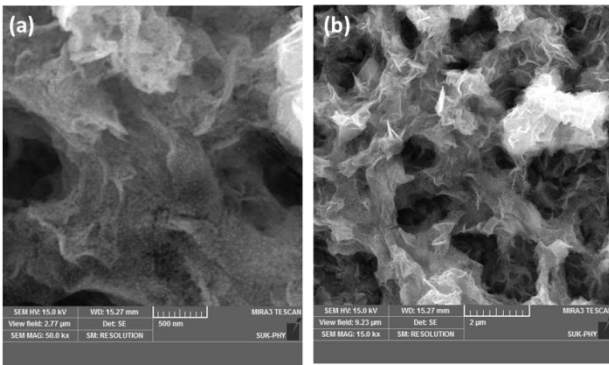


Fig. 2 – XRD pattern of the Mn_2O_3 electrode

Fig. 3 shows the FTIR spectra of the Mn_2O_3 thin film that is used to confirm the formation of Mn_2O_3 by potentiostatic electrodeposition. The two sharp peaks appearing at 561 and 676 cm^{-1} are assigned to the Mn–O–Mn asymmetric stretching and stretching vibration of Mn–O units, respectively [10]. The peaks at 1218 and 1339 cm^{-1} can be assigned to the Mn=O stretching vibrations. The peaks at about 3242 and 1695 cm^{-1} can be assigned to O–H stretching and bending vibrations of H_2O molecules adsorbed on the surface of Mn_2O_3 nanoparticles, respectively [11].

Fig. 4a and Fig. 4b show FESEM images of potentiostatically electrodeposited Mn_2O_3 thin film prepared at 500°C at two different magnifications of 500 nm and $2 \mu\text{m}$, respectively. It can be seen that the nanoflake or lamellar morphology covers the surface of the SS substrate. This kind of morphology is suitable for active materials for better electrochemical performance [12]. Moreover, visible voids can be observed between clusters of nanoflakes, thereby offering a large contact surface between the electrolyte and active materials. These voids in materials may be a detrimental factor of the porosity of the materials [13].

Fig. 3 – FTIR spectra of the Mn_2O_3 electrodeFig. 4 – FESEM images of the Mn_2O_3 electrode: (a) 500 nm, (b) 2 μm magnification

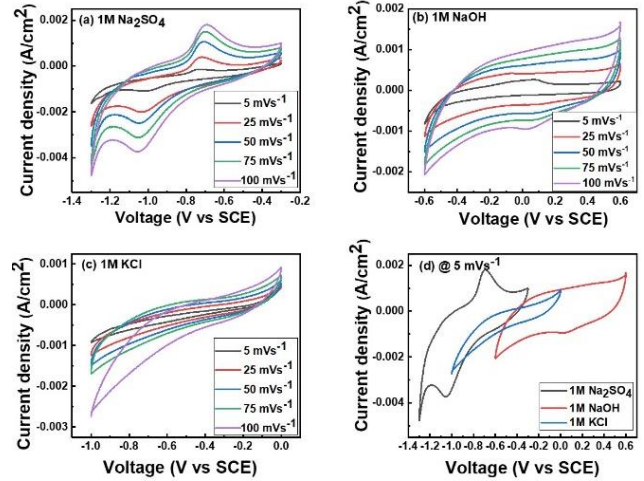
The electrochemical performance of potentiostatically deposited Mn_2O_3 nanoflake type SC electrode annealed at 500 °C was studied using cyclic voltammetry (CV), galvanostatic charge/discharge (GCD), and AC impedance measurements (EIS) in 1 M NaOH, 1 M Na_2SO_4 and 1 M KCl electrolytic solutions. In a three-electrode system, the Mn_2O_3 electrode was used as the working electrode, SCE as the counter electrode and a platinum wire as the counter electrode. In each electrolyte, the cyclic voltammetry scanned at different scan rates from 5 to 100 mVs^{-1} in a suitable potential window, as shown in Fig. 5a-c. In connection to the variation in scan rates, the fabricated Mn_2O_3 electrode exhibits the oxidation-reduction pair peaks with varied charge-discharge curve geometries. The findings point to an electrolyte over the Mn_2O_3 electrode as the source of the faradaic pseudocapacitance. A faradaic redox reaction can also be attributed to the well-defined oxidation reduction pair peaks [14].

The specific capacitance C_{sp} was calculated using the following expression:

$$C_{sp} = \frac{A}{mk\Delta V}, \quad (2)$$

where A is the integral area of the cyclic voltammogram loop, ΔV is the sweep potential window, k is the scan rate (dv/dt), and m is the mass of the electrode material on each electrode [15]. As seen in Fig. 5d, Mn_2O_3 electrode-based supercapacitor shows a high C_{sp} of 508 Fg^{-1} in 1 M Na_2SO_4 solution at 5 mVs^{-1} scan

rate. It is observed that the area under the CV curve for Na_2SO_4 is higher than that of NaOH and KCl electrolytes, suggesting the higher specific capacitance of Mn_2O_3 electrodes [16]. The C_{sp} values for 1 M Na_2SO_4 , 1 M NaOH and 1 M KCl electrolytic solutions are presented in Table 1.

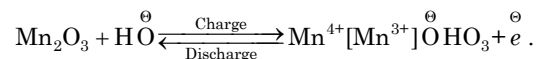
Fig. 5 – CV curves of the Mn_2O_3 electrode at 5–100 mVs^{-1} scanning rate: (a) 1 M Na_2SO_4 , (b) 1 M NaOH, (c) 1 M KCl and (d) CV curves of Mn_2O_3 electrode at 100 mVs^{-1} scanning rate in 1 M Na_2SO_4 , 1 M NaOH and 1 M KClTable 1 – C_{sp} values of the Mn_2O_3 electrode in various electrolytes at a scan rate of 5 mVs^{-1}

Sr. No.	Electrolyte	Specific capacitance C_{sp} , Fgm^{-1}
1	1 M Na_2SO_4	508
2	1 M NaOH	331
3	1 M KCl	189

The better C_{sp} values may be attributed to an increase in the surface area, porous surface, and homogeneity, which facilitates the creation of large active sites and rapid ionic transport across the Mn_2O_3 electrode surface. A porous structure, in particular, can provide a large and accessible surface area for ion adsorption, improving cation accessibility and shortening the ion diffusion path [17, 18].

The values of C_{sp} for the Mn_2O_3 electrode in 1 M Na_2SO_4 , 1 M NaOH and 1 M KCl at different scan rates from 5 to 100 mVs^{-1} are shown in Fig. 6a. It is observed that C_{sp} values decrease because at higher scan rates, inner active sites are not involved in redox transitions. Thus, it can be assumed that, at low scan rates, C_{sp} almost completely utilize the electrode material.

In general, an oxidation reaction occurs in an electrochemical process to convert Mn^{3+} to Mn^{4+} in Mn_2O_3 electrode. Through chemisorption and/or intercalation, this oxidation process generally enhances the kinetics of the OH⁻/Cl⁻ reaction (in the case of NaOH and KCl electrolytes) over the Mn_2O_3 cubic lattice. The following electrochemical reaction, which involves chemisorption/intercalation of OH⁻/Cl⁻ over Mn_2O_3 surfaces, can explain the charge/discharge mechanism [19]:



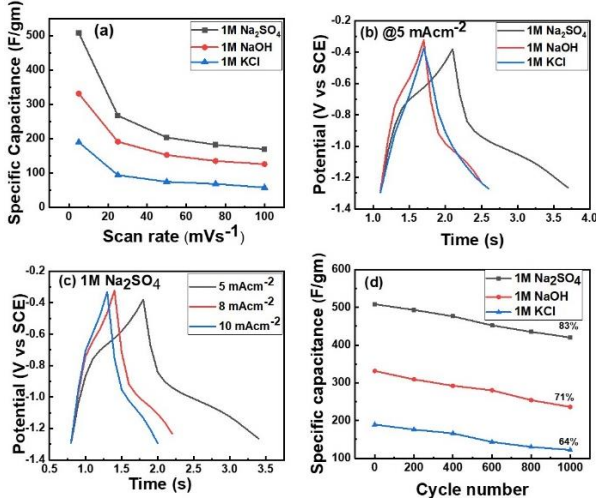
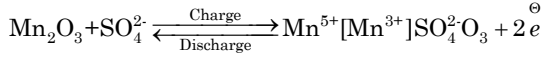


Fig. 6 – (a) Variation of C_{sp} values of Mn_2O_3 at different scan rates in three electrolytes; (b) GCD measurements at a current density of 5 mAcm^{-2} in three electrolytes; (c) GCD measurements at different current densities in $1 \text{ M Na}_2\text{SO}_4$ electrolyte; (d) stability of the Mn_2O_3 film over 1000 cycles at a scan rate of 100 mVs^{-1}

Chemisorption/intercalation of SO_4^{2-} over Mn_2O_3 surfaces, production of Mn^{3+} to Mn^{5+} in the Mn_2O_3 electrode, and the charge/discharge mechanism in the case of Na_2SO_4 electrolyte might be explained by the following reaction:



3.4.2. Galvanostatic Charge-Discharge (GCD) Analysis

The GCD behavior of the potentiostatically electro-deposited Mn_2O_3 electrode prepared at 500°C is investigated in $1 \text{ M Na}_2\text{SO}_4$, 1 M NaOH and 1 M KCl electrolytes using chronopotentiometric technique at a current density of 5 mAcm^{-2} in the potential windows -1 to -0.38 V , -1 to -0.32 V and -1 to -0.36 V , respectively. The charge/discharge behavior is shown in Fig. 6b. Even if charging/discharging processes have a triangle form, potential time responses are not totally linear like carbon-based supercapacitors following a typical pseudocapacitance pattern. The Mn_2O_3 electrode displays improved capacitive and stability performance in $1 \text{ M Na}_2\text{SO}_4$ electrolyte among the electrolyte systems chosen for studies, therefore charge/discharge measurements are undertaken to obtain additional information at various current densities of 5, 8, 10 mAcm^{-2} , as shown in Fig. 6c. The material has a longer discharge time when the current density is low, and a shorter discharge time when the current density is high. The exponential behavior of the time-dependent discharge curve suggests typical pseudocapacitive behavior, which is caused by an electrochemical redox reaction at the electrode/electrolyte interface [20].

The supercapacitor electric parameters such as specific energy (SE) and specific power (SP) were calculated from the relations [20]:

$$SE = \frac{VI_d t_d}{m}, \quad (3)$$

$$SP = \frac{VI_d}{m}, \quad (4)$$

where I_d and t_d are the current density and discharge time, respectively, m is the mass of active material within the Mn_2O_3 electrode.

The values of specific energy (SE) and specific power (SP) of potentiostatically electro-deposited Mn_2O_3 electrodes were calculated from GCD in 1 M electrolytes of Na_2SO_4 , NaOH and KCl at 5 mAcm^{-2} and are listed in Table 2. The nanoflake type Mn_2O_3 electrode shows higher specific energy and specific power values in Na_2SO_4 compared to NaOH and KCl electrolytes.

Table 2 – Specific energy (SE) and specific power (SP) of Mn_2O_3 electrodes at 1 M concentration in different electrolytes

Sr. No.	Electrolyte	SE (Wh/kg)	SP (kW/kg)
1	Na_2SO_4	44.72	41.66
2	NaOH	22.19	30.26
3	KCl	24.83	40.13

3.4.3. Electrochemical Stability Analysis

The long-term electrochemical stability of the Mn_2O_3 nanoflake type electrode was investigated in different electrolytes using a CV test at a scan rate of 100 mVs^{-1} to further evaluate the performance of the Mn_2O_3 electrode. Fig. 6d depicts the stability of the Mn_2O_3 nanoflake type electrode in $1 \text{ M Na}_2\text{SO}_4$, 1 M NaOH , and 1 M KOH electrolytes over 1000 cycles at a scan rate of 100 mVs^{-1} , with capacity retention values of 83, 71, and 64 %, respectively.

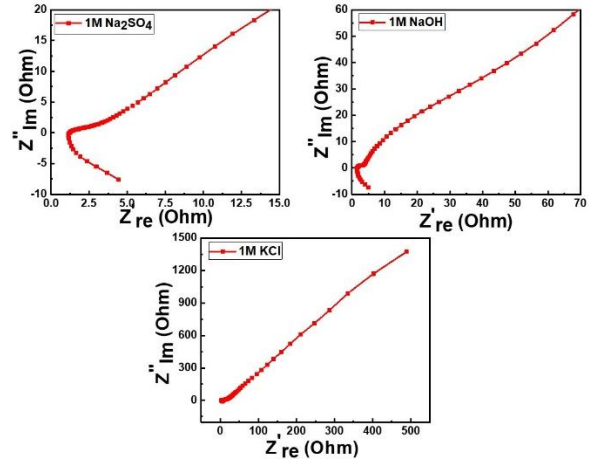


Fig. 7 – Nyquist plots of the Mn_2O_3 electrode in 1 M electrolytes: (a) Na_2SO_4 (b) NaOH and (c) KCl

When compared to other electrolytes, the Na_2SO_4 electrolyte exhibits low capacitance loss; hence, Na_2SO_4 may be regarded as a more stable electrolyte for the Mn_2O_3 nanoflake-type electrode. The capacitance loss may be due to the composition damage caused by irreversible chemical processes and mechanical stress to the electrode material's physical structure caused by the intercalation/deintercalation of electrolyte ions during charge/discharge cycles to counterbalance the total charge. A repetitive charge/discharge cycle will almost certainly result in mechanical and electrical issues, lowering the initial performance due to the loss of the

active material mass.

To study conductivity and electrochemical reactions, EIS analyses were accomplished which is a vital tool to examine frequency performance. Fig. 7 reveals the Nyquist plot of the Mn_2O_3 electrode in 1 M Na_2SO_4 , NaOH and KCl electrolytes. The Nyquist plot consists of a semicircle at high frequencies and a straight line at low frequencies.

4. CONCLUSIONS

The potentiostatic electrodeposition technique was adopted to synthesize nanoflake type Mn_2O_3 supercapacitor electrode. The XRD analysis revealed the BCC crystal structure with a crystallite size of 17.27 nm. Nanoflake, lamellar and porous morphology was observed from FESEM, offering a large contact surface between the electrolyte and active material necessary

for better electrochemical properties. The Mn_2O_3 nanoflake type electrode in 1 M Na_2SO_4 has excellent electrochemical performance bearing specific capacitance of 508 Fg^{-1} at a scan rate of 5 mVs^{-1} , specific energy of 44.72 Wh/kg , specific power of 41.66 kW/kg and electrochemical stability of 83 % after 1000 cycles demonstrating the suitability of material for supercapacitor device fabrication.

ACKNOWLEDGEMENTS

The author (SGP) is thankful to D.B.F. Dayanand College of Arts and Science for the financial support through the Start-up grant scheme No. DAYA/MAS-RSG/01. The corresponding author (IAD) is thankful to Sadguru Gadage Maharaj College, Karad for financial support through RUSA Ref. No. SGM/RUSA/MRP/F. No-4, 253/2020-21.

REFERENCES

1. Y. Wang, Z. Shi, Y. Huang, Y. Ma, C. Wang, M. Chen, Y. Chen, *J. Phys. Chem. C* **113**, 13103 (2009).
2. J.R. Miller, P. Simon, *Science* **321**, 651 (2008).
3. I.A. Dhole, Y.H. Navale, C.S. Pawar, S.T. Navale, V.B. Patil, *J. Mater. Sci.: Mater. Electron.* **29**, 5675 (2018).
4. M. Yaseen, M.A.K. Khattak, M. Humayun, M. Usman, S.S. Shah, S. Bibi, B.S. Ul Hasnain, S.M. Ahmad, A. Khan, N. Shah, A.A. Tahir, H. Ullah, *Energies* **14**, 7779 (2021).
5. N. Sui, Y. Duan, X. Jiao, D. Chen, *J. Phys. Chem. C* **113**, 8560 (2009).
6. M.S. Kolathodi, S.N.H. Rao, T.S. Natarajana, G. Singh, *J. Mater. Chem. A* **4**, 7883 (2016).
7. M. Zhang, D. Yang, J. Li, *Vacuum* **178**, 109455 (2020).
8. B. Xu, S. Yue, Z. Sui, X. Zhang, S. Hou, G. Cao, Y. Yang, *Energy Environ. Sci.* **4**, 2826 (2011).
9. J.B. Thorat, N.S. Harale, I.A. Dhole, S.K. Shinde, M.C. Rath, T.J. Shinde, N.S. Shinde, V.J. Fulari, *J. Mater. Sci.: Mater. Electron.* **32**, 20031 (2021).
10. B. Gillot, M.E. Guendouzi, M. Laarj, *Mater. Chem. Phys.* **70**, 54 (2001).
11. M. Salavati-Niasari, M. Esmaeili-Zare, M. Gholami Daghighian, *Adv. Powder Technol.* **25**, 879 (2014).
12. S.M. Ingole, S.T. Navale, Y.H. Navale, I.A. Dhole, R.S. Mane, F.J. Stadler, V.B. Patil, *J. Solid State Electron. Chem.* **21**, 1817 (2017).
13. M. Demir, B. Ashourirad, J.H. Mugumya, S.K. Saraswata, H.M. El-Kaderi, R.B. Gupta, *Int. J. Hydrog. Energy.* **43**, 18549 (2018).
14. M. Toupin, T. Brousse, D. Bélanger, *Chem. Mater.* **16**, 3184 (2004).
15. M. Salari, S.H. Aboutalebi, K. Konstantinov, H.K. Liu, *Phys. Chem. Chem. Phys.* **13**, 5038 (2011).
16. T.P. Gujar, W. Kim, I. Puspitasari, K.D. Jung, O.S. Joo, *J. Electrochem. Sci.* **22**, 666 (2007).
17. I.K. Gopalakrishnan, N. Bagkar, R. Ganguly, S.K. Kulshreshtha, *J. Cryst. Growth* **280**, 436 (2005).
18. Z.Y. Li, M.S. Akhtar, P.T.M. Bui, O.B. Yang, *Chem. Eng. J.* **330**, 1240 (2017).
19. Y.H. Son, T.M. Phuong Bui, H.R. Lee, M.S. Akhtar, D.K. Shah, O.B. Yang, *Coatings* **9**, 631 (2019).
20. I.A. Dhole, M.M. Tonape, U.T. Pawar, S.S. Gavande, S.G. Pawar, V.B. Patil, *Macromolec. Symposia* **387**, 1800212 (2019).

Електрохімічна поведінка чистих ефективних електродів Mn_2O_3 , отриманих за недорогою технікою потенціостатичного електроосадження

S.G. Pawar¹, C.V. Chanmal¹, S.S. Bandgar¹, R.N. Mulik¹, P.A. Desai², A.A. Admuthe², I.A. Dhole³

¹ Department of Physics, D.B.F. Dayanand College of Arts and Science, 413002 Solapur, (M.S.), India

² Department of Physics, Smt. Kasturbai Walchand College, 416416 Sangli, (M.S.), India

³ Department of Physics, Sadguru Gadage Maharaj College, 415124 Karad, (M.S.), India

Електрод типу нанолусок з Mn_2O_3 для застосування в суперконденсаторах був успішно електроосаджений на колектор струму з нержавіючої сталі (SS) потенціостатичним способом без використання будь-якого сполучного або закупорювального засобу. Структурні, морфологічні та композиційні властивості підготовлених електродів Mn_2O_3 були охарактеризовані за допомогою методів дифракції рентгенівських променів (XRD), польової емісійної скануючої електронної мікроскопії (FESEM) та інфрачервоної спектроскопії з перетворенням Фур'є (FTIR) відповідно. Дослідження XRD виявило наночастинки Mn_2O_3 , які мають кристалічну об'ємно-центровану кубічну структуру (BCC), підтверджену за допомогою JCPDS no. 89-2809. Зображення FESEM демонструють морфологію нанолусок, а також пластинчасту та пористу морфологію, придатну для електрохімічних застосувань. Утворення Mn_2O_3 було підтверджено за допомогою FTIR спектрів. Електрохімічні характеристики електроду Mn_2O_3 досліджували за допомогою циклічної вольтамперометрії (CV), гальваностатичного заряду/розряду (GCD) та електрохімічної імпедансної спектроскопії (EIS) в електролітах Na_2SO_4 , NaOH та KCl. Виявлено, що електроліт 1 M Na_2SO_4 добре підходить для електроду типу нанолусок з Mn_2O_3 для застосування в суперконденсаторах з питомою ємністю (C_{sp}) 508 Fg^{-1} при швидкості сканування 5 mVs^{-1} .

Кращі значення C_{sp} можуть бути пов'язані з великими активними центрами та швидким іонним транспортом через поверхню електрода Mn_2O_3 . Аналіз електрохімічної стабільності електрода Mn_2O_3 показує збереження ємності 83 % після 1000 циклів в електроліті 1 M Na_2SO_4 при швидкості сканування 100 мВс^{-1} .

Ключові слова: Mn_2O_3 , Циклічна вольтамперометрія, Суперконденсатор, Електроосадження.